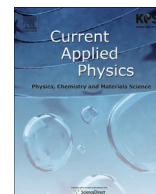




Contents lists available at ScienceDirect

Current Applied Physics

journal homepage: [www.elsevier.com/locate/cap](http://www.elsevier.com/locate/cap)

## Enhanced and broadband absorber with surface pattern design for X-Band

Chenguang Wu<sup>a, b, c</sup>, Shuwen Chen<sup>b, c</sup>, Xisheng Gu<sup>b, c</sup>, Renchao Hu<sup>b, c</sup>, Shuomin Zhong<sup>d</sup>, Guoguo Tan<sup>b, c, \*</sup>, Qikui Man<sup>b, c, \*\*</sup>, Chuntao Chang<sup>b, c</sup>, Xinmin Wang<sup>b, c</sup>, Run-Wei Li<sup>b, c</sup>

<sup>a</sup> Nano Science and Technology Institute, University of Science and Technology of China, Suzhou, Jiangsu 215123, China

<sup>b</sup> Key Laboratory of Magnetic Materials and Devices, Ningbo Institute of Materials Technology & Engineering, Chinese Academy of Sciences, Ningbo, Zhejiang 315201, China

<sup>c</sup> Zhejiang Province Key Laboratory of Magnetic Materials and Application Technology, Ningbo Institute of Materials Technology & Engineering, Chinese Academy of Sciences, Ningbo, Zhejiang 315201, China

<sup>d</sup> Faculty of Electrical Engineering and Computer Science, Ningbo University, Ningbo, Zhejiang 315211, China

### ARTICLE INFO

#### Article history:

Received 19 April 2017

Received in revised form

12 October 2017

Accepted 17 October 2017

Available online xxx

#### Keywords:

Microwave absorber

Surface pattern design

Broadband

Carbonyl iron

### ABSTRACT

A broadband and thin-layer microwave absorber is designed based on surface pattern design made by carbonyl iron and rubber composite. The bandwidth with reflection less than  $-10$  dB covers the full X-band owing to two absorption peaks appeared simultaneously in both the simulation results and experimental results. In this work, the power loss and power flow diagram were present by CST simulation, which clearly explain the broadband absorption caused by double  $\lambda/4$  matching absorption and interfacial scattering synergistic effect. A facile splicing method was provided to extend the absorption bandwidth for the magnetic absorbing materials.

© 2017 Elsevier B.V. All rights reserved.

### Contents

1. Introduction .....	00
2. Simulation methods and experiments .....	00
3. Results and discussion .....	00
4. Conclusions .....	00
Acknowledgments .....	00
References .....	00

\* Corresponding author. Key Laboratory of Magnetic Materials and Devices, Ningbo Institute of Materials Technology and Engineering, Chinese Academy of Sciences, No. 1219 Zhongguan West Road, Zhenhai District, Ningbo 315201, PR China.

\*\* Corresponding author. Key Laboratory of Magnetic Materials and Devices, Ningbo Institute of Materials Technology and Engineering, Chinese Academy of Sciences, No. 1219 Zhongguan West Road, Zhenhai District, Ningbo 315201, PR China.

E-mail addresses: [kant01@126.com](mailto:kant01@126.com) (G. Tan), [manqk@nimte.ac.cn](mailto:manqk@nimte.ac.cn) (Q. Man).

<https://doi.org/10.1016/j.cap.2017.10.012>

1567-1739/© 2017 Elsevier B.V. All rights reserved.

### 1. Introduction

Microwave absorbing materials (MAMs) have wide applications in civilian and modern military areas such as electromagnetic interference (EMI) protection, antenna and electromagnetic wave stealth [1–5]. Broad absorption bandwidth is critical to evaluate MAMs since electromagnetic device and military radar work in a wide frequency range [6].

Generally, the microwave absorption performance depends on its complex permittivity ( $\epsilon_r = \epsilon' - j\epsilon''$ ), complex permeability ( $\mu_r = \mu' - j\mu''$ ), sample thickness and frequency range [7]. However,

suffering from the Snoek's limit [8,9], it is difficult to further increase the permeability for magnetic material in higher frequency. Hence, the loss mechanisms such as magnetoelectric control [10,11], multiple reflections effect [12,13] or resonance absorption [14,15] are inevitable to broaden the magnetic materials absorption bandwidth. Wan et al. [16] synthesized FeCo-coated carbon fibers to regulate permeability for magnetoelectric control, the permittivity and the permeability can be well matched at high frequencies, the absorption bandwidth of reflection loss (RL) below  $-10$  dB is about 2.5 GHz with absorber thicknesses of 1.3–1.5 mm. Furthermore, the multiple reflections of electromagnetic waves in the absorber are also used to design broadband absorbing material. Due to the extension of electromagnetic waves' propagation path, the power loss of electromagnetic waves can be effectively increased. The bandwidth of natural microcrystalline graphite/low density polyethylene (MG/LDPE) composites with RL less than  $-10$  dB reaches 3.02 GHz at the thickness of 2.0–2.1 mm [7]. Taking advantage of the emerging concept of metamaterials, Li et al. [17] provided an ultra-broadband microwave hybrid absorber, which shows 90% absorption over 2–18 GHz with the effective thickness of 21 mm. However, broadband absorbing materials designed by above methods are either not wide enough or hard to mold, which greatly restricts the applications in practice.

In this work, a facile splicing method was proposed to design a broadband and thin-layer microwave absorber in order to overcome the problem of narrow absorption bandwidth for single  $\lambda/4$  matching absorption due to the thickness sensitivity. The designed parameters are optimized using a frequency domain solver, implemented by CST MWS. The broadband microwave absorber was fabricated and RL was measured. The RL below  $-10$  dB covers the whole X-band and the experimental results agree well with the simulation results. Finally, broadband characteristics and loss mechanisms of the absorber were discussed in details.

## 2. Simulation methods and experiments

The broadband absorption properties of the former designed MAM are demonstrated by numerical simulations using a commercial finite-element-method (FEM) by CST MWS simulation software. Based on waveguide as the perfect conductor, ideal electricity boundary is set around the MAMs. The size of the absorbing material was determined by the port size of standard X-band waveguide, and the sketch map of waveguide and the absorber were shown in Fig. 1(a) and (b), respectively.

The carbonyl iron particles (CIs) were uniformly dispersed in the mixed rubber with a volume percentage of 35%, and the mixed rubber was composed of styrene-butadiene rubber (SBR) and PU by

mass ratio of 3:1. CIs, SBR and PU were mixed directly (Cyclohexanone was used to solvent), then the mixture was taken uniformly under ultrasonic stirring for 8 h, and absorbing film was obtained by tape casting method. Finally, the absorber with a stepped structure was obtained by hot pressing method.

The phase was examined by X-ray diffraction (XRD, Bruker AXS) using Cu-K $\alpha$  radiation. The morphology was analyzed by scanning electron microscope (SEM, Hitachi S-4800). The complex permeability of these composite samples were obtained by using an Agilent N5225A vector network analyzer in the 0.1–18 GHz.

## 3. Results and discussion

The phase and morphologies of CIs were observed by XRD and SEM, respectively. Fig. 2(a) shows the diffraction pattern for CIs which has three narrow peaks at  $44.7^\circ$ ,  $65.0^\circ$  and  $82.3^\circ$  corresponding to (110), (200), and (211) of  $\alpha$ -Fe, respectively. The integrated characterizations of the as-obtained typical spherical CIs as shown in Fig. 2(b), and the quantitative analysis (inset Figure) presents the diameter of the CI particles, which measured on average  $0.9 \mu\text{m}$ , ranges from  $0.1$  to  $3 \mu\text{m}$ .

Fig. 3(a) gives the complex permittivity ( $\epsilon_r = \epsilon' - j\epsilon''$ ) and complex permeability ( $\mu_r = \mu' - j\mu''$ ) values of the CI/rubber composite at frequency range of 0.1–18 GHz, including their real part and imaginary part. The permittivity is almost consent in the entire frequency range, and the permeability imaginary part ( $\mu''$ ) has a rising trend after 1 GHz. As a comparison between complex permittivity and complex permeability in the entire measurement range, though  $\epsilon_r$  is larger than  $\mu_r$ , the magnetic loss tangent ( $\tan\delta_m = \mu''/\mu'$ ) is larger than the dielectric loss tangent ( $\tan\delta_e = \epsilon''/\epsilon'$ ), which explains that CI is a typical magnetic loss material, as shown in Fig. 3(b).

In order to characterize the electromagnetic wave absorption performance of the single-layer CI/rubber composite, the RL curves at different absorber thickness are calculated by using Eqs. (1) and (2) according to transmission-line theory [18].

$$Z_{\text{in}} = Z_0 \sqrt{\frac{\mu_r}{\epsilon_r}} \tanh \left[ j \left( \frac{2\pi f t}{c} \right) \sqrt{\mu_r \epsilon_r} \right] \quad (1)$$

$$\text{RL}(\text{dB}) = 20 \lg \left| \frac{Z_{\text{in}} - Z_0}{Z_{\text{in}} + Z_0} \right| \quad (2)$$

Where  $Z_{\text{in}}$  represents impedance of the composite,  $Z_0$  is intrinsic impedance of free space,  $\mu_r$  and  $\epsilon_r$  are the complex permeability and complex permittivity.  $f$  represents frequency,  $t$  represents the absorber thickness,  $c$  represents velocity of light in free space. Fig. 4 shows the frequency dependence of RL of the CI/rubber composite samples at three different thicknesses. It can be found that the absorption peak moves to lower frequency with the increase of thickness, and the absorption peak frequency and intensity strongly depends on the absorber thickness. The  $\lambda/4$  cancellation theory has been frequently employed to explain this phenomenon [19,20]. Here, the bandwidth is defined as the frequency width in which the absorption is less than  $-10$  dB. When the thickness is 1.9 mm, the bandwidth is the widest. However, it is worth noting that the absorber with a thickness of 1.9 mm has RL values exceeding  $-10$  dB in the 8.3–11.7 GHz range, as well as the bandwidth below  $-15$  dB is only 1.8 GHz.

The patterned absorber is designed and fabricated as a stepped structure as shown in Fig. 1(b). The patterned absorber consists of two units with sizes of  $l_x \times 10.1 \text{ mm} \times 1.7 \text{ mm}$ ,  $(22.8 \text{ mm} - l_x) \times 10.1 \text{ mm} \times 2.1 \text{ mm}$ , respectively. By changing the value of  $l_x$ , the relationship between  $l_x$  and the bandwidth of MAMs can be gained, as shown in Fig. 5. The bandwidth with RL  $< -10$  dB

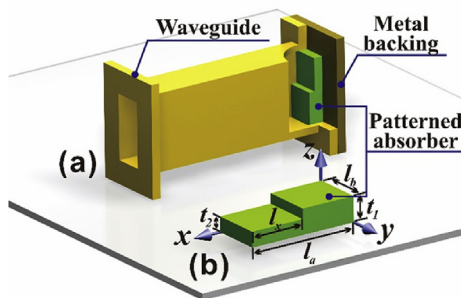


Fig. 1. (a) Schematic 3D view of the patterned absorber in X-band waveguide for simulation and measurement. (b) Enlarged view of the absorber with  $l_x = 22.8 \text{ mm}$ ,  $l_y = 10.1 \text{ mm}$ ,  $t_1 = 2.1 \text{ mm}$  and  $t_2 = 1.7 \text{ mm}$ .

Download English Version:

<https://daneshyari.com/en/article/8148175>

Download Persian Version:

<https://daneshyari.com/article/8148175>

[Daneshyari.com](https://daneshyari.com)